Experimental investigation of the aluminum combustion in different O2 oxidizing mixtures: Effect of the diluent gases

Alexandre Braconnier, Christian Chauveau, F. Halter, S. Gallier

Experimental investigation of the aluminum combustion in different O_2 oxidizing mixtures: effect of the diluent gases

A. Braconnier[a]*, C. Chauveau[b], F. Halter[b] and S. Gallier[a]

[a] ArianeGroup, CRB, 9 rue Lavoisier, 91710 Vert-Le-Petit, France
[b] ICARE-CNRS, 1C avenue de la recherche scientifique 45071 Orléans Cedex, France
* Corresponding author.
E-mail address: alexandre.braconnier@cnrs-orleans.fr

Abstract

The existence of different distinct phases during the aluminum combustion process was unambiguously proved and widely discussed in several studies on single burning aluminum particles. Indeed, in the case of a combustion in diffusion vapor phase, the formation of growing aluminum oxide caps on the droplet surface is suspected to drive the transition from a symmetric to an asymmetric regime. Especially based on diverse observations for aluminum particles burning in O_2/N_2, a hypothesis was proposed on the effect of N_2 which probably contributes to the regime transition occurrence. To extend research efforts and get a further understanding of the asymmetric transition development, and, more generally on aluminum combustion, an analysis in O_2/N_2, O_2/Ar and O_2/He oxidizing mixtures is presented. This work is based on an advanced experimental technique allowing to levitate a single particle and visualize its self-sustained combustion with high temporal and spatial resolution. Combustion parameters of ignited micron-sized aluminum particles (30 to 100 µm) at atmospheric pressure were accurately determined using optical diagnostics. Results provide a new quantified dataset and allow to compare the relative effect of N_2, Ar and He as diluent gases in the aluminum combustion process. Burning times are found to be similar, regardless of the considered diluent gas, as well as the aluminum consumption rate in symmetric regime. However, estimations on the relative duration of the symmetric phase demonstrate a potential influence of N_2 which promotes the regime transition in comparison with Ar and He for low molar fraction of oxidizer. The ratio between flame and droplet diameters is also modified depending on the inert gas and is determined. Observed trends are discussed and compared to available data to improve the description and quantification of the relative influence of the inert gases.

Keywords: Aluminum combustion; Experimental characterization; Solid propulsion.

1. Introduction

Since many years, energetic materials used in solid rocket motors (SRM) contain aluminum micron-sized particles. Especially useful to increase temperatures and thrust, burning aluminum particles are also suspected to drive damaging thermo-acoustic instabilities inside SRM [1]. In addition, incomplete aluminum combustion could result in performance loss. Thus, the understanding of the aluminum combustion process in representative SRM conditions is required to improve predictive models and ensure motor reliability and performance.

Micro-sized aluminum particles react inside the SRM chamber, near the solid propellant surface [2]. Surrounding ambient environment is composed of various oxidizers such as CO, H_2O and CO_2 but an important proportion of inert gas N_2 can also be found. Inert gas N_2 is suspected to participate to the transition from symmetric to asymmetric phase during the aluminum combustion process as suggested by Dreizin [3] and recently accurately observed [4] through studies on single burning aluminum particles.

The existence of different combustion modes was first identified on burning aluminum samples in a flat propane/oxygen flame with additional N_2 flow [5]. Authors observed distinct

aluminum combustion behaviors, with and without fragmentation of the aluminum particles. Fragmentation occurrence is attributed to the partial pressure of oxygen and this mode is presented as more rapid and also more complete [5]. The effects of the inert gases N_2 and Ar on the combustion process were directly investigated [6]. Observations made on freely falling droplets report differences on particles trajectories and on light emission traces, with vigorous spinning / jetting and irregular emissions in the case of particles burning in air. Analysis of quenched droplets has also shown non-symmetric smoke patterns with an important hemispherical aluminum oxide lobe for droplets ignited in air. Important light or trajectory variations as well as agglomeration of oxide on droplet surface were not identified with combustion in O_2/Ar. Assumption that accumulation of aluminum oxide on the surface can explain the variation in the combustion behavior has been established [6].

Based on this conclusion, several studies were conducted and focused on determining the accumulation process of oxide on the burning droplet surface and the effect of N_2 [3, 7-9]. Relying on experimental results, a detailed mechanism was proposed, considering that gaseous suboxides are formed in the flame during intermediate reactions and diffuse to the liquid droplet surface before being dissolved in the aluminum, modifying aluminum boiling point and therefore, liquid droplet temperature. Then, depending on the equilibrium binary Al-O phase diagram, heterogeneous reactions can produce oxygen-containing species on droplet surface, independently of the diluent gas. In the case of aluminum burning in O_2/N_2, the formation of intermediate NO can contribute to additional oxygen diffusion to the particle, accelerating the oxide lobe growth.

Existence of NO species was supported by SEM and X-ray analysis [10], however data highlighting the relative N_2 effect on combustion parameters are scarce, requiring to be completed. The few available data reported that combustion times, combustion rates and flame sizes, both in N_2 or Ar diluted with dry or wet oxidizers, are similar [11-13]. The widely-used Beckstead's correlation estimating the combustion time of an isolated burning aluminum particle [14] deviates from the theoretical D^2 model determined for evaporation of liquid fuel droplets [15]. Combustion time is given to depend on the initial particle diameter as $D_0^{\,n}$ with a reduced burning time exponent $n \sim 1.8$. Several parameters are also considered such as ambient temperature and pressure as well as the oxidizer proportions and efficiency. Nonetheless, according to global observations, even if the burning time seems independent of the diluent gas, the non-consideration of a potential diluent efficiency in this correlation has to be validated. Indeed, diffusion of species drives reactions in the diffusion mode and the influence of inert gases properties (heat capacity, mass diffusivity, etc.) is not established despite its potential effect. Information on this aspect could improve our current understanding of the various phenomena that lead to the regime transition and combustion process of aluminum.

This work addresses the combustion of single levitated aluminum particles, varying dilution conditions (type of inert gas and proportions) in O_2 at atmospheric pressure. Particle size is selected to be representative of the particle size initially used solid propellants to the typical size of aluminum agglomerates in SRM (30 to 120 µm). An advanced experimental set-up is proposed, allowing to characterize droplet combustion process in static and controlled gaseous environments. Optical diagnostics allow high temporal and spatial resolution to finely evaluate combustion parameters and interaction mechanisms between aluminum and its oxide. This study is devoted to providing new and more accurate experimental data, especially on the effect of the diluent gases using latest imaging technologies.

2. Experimental set-up

The results presented in this paper are based on the experimental apparatus used and detailed in a previous study on aluminum combustion [4]. Thus, an electrodynamics levitator (EDL) is used to isolate a single aluminum particle in an electric field without any perturbing physical

mean. Confinement in a high pressure chamber allows creating a static gaseous environment to prevent from convective effects while controlling the ambient conditions in terms of pressure and composition. Molar composition is controlled by a high pressure gauge, using partial pressures. Schematic representation of the apparatus is represented in Fig. 1.

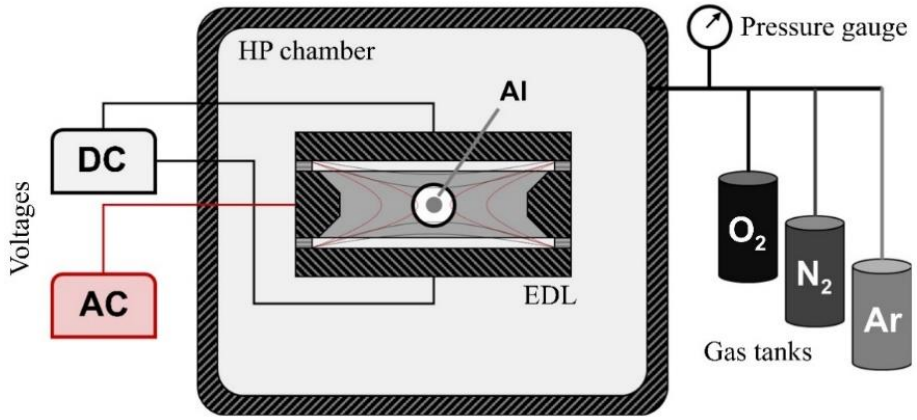

Figure 1. Schematic representation of the experimental apparatus

Once ambient conditions are fixed, aluminum particles are charged by triboelectric effect in the injector and injected inside the EDL. A particle cloud is firstly formed in the EDL and a single sample is then isolated by adjusting voltages parameters. Hence, the electric field is used to set a reproducible initial position of the particle. Then, considerable charge losses occur at high temperature by thermoionic emission during combustion [3] and prevent from any influence of the electric field on condensed species. Several tests were conducted on this issue and corroborate this assumption. Moreover, despite possible ionization in the flame, axisymmetric geometry of the electric field inside the EDL preserves combustion from any preferential and perturbing electric effect on the reacting zone.

Combustion is ignited by a separated and focused CO_2 laser beam as shown in Fig. 2. Measurements are mainly based on optical diagnostics. First, filtered photomultipliers tubes (PM) are used to transform the light emission collected during combustion into voltage signals and a trace of the light intensity is recorded (Fig. 2). The CO_2 laser is synchronized with a photomultiplier signal and its extinction is triggered when the luminous emission from the heated particle exceeds a defined threshold, ensuring the self-sustained combustion of the aluminum droplet. A high-speed camera PHANTOM V1611 combined with a long-distance microscope QUESTAR QM100 is also focused on the single burning particle (Fig. 2). Dynamics sequences are recorded with high temporal and spatial resolution (up to 40000 fps for 1.7 - 2.5 µm/px) and a fine evolution of the combustion parameters is determined. The camera recording is coupled to the laser trigger which is the temporal origin.

Initial droplet diameter and temporal evolution of the droplet/flame diameters are determined by a home-made Matlab processing routine based on intensity profile analysis. Combustion time is defined as the duration between ignition and extinction. Ignition is directly identified on the videography from the high-speed camera, coinciding to the time of the first picture where the diffusion flame takes place around the melted aluminum particle. Extinction corresponds to the end of the combustion process and is considered when the intensity of the photomultiplier signal recovers its initial value. Thus, the burning time is calculated using synchronized information of the high-speed camera and photomultipliers respectively determined with image processing and signal processing.

More detail on the set-up and post-processing can be found in [4].

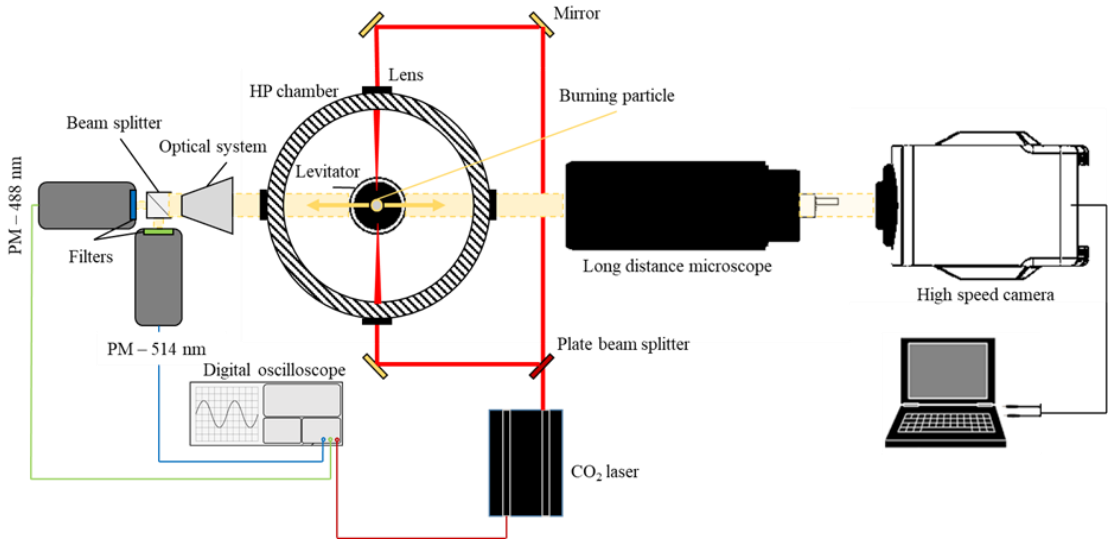

Figure 2 . Schematic representation of the experimental setup

3. Results

3.1. Combustion time

The combustion time could be a direct indicator of the influence of the ambient composition and was consistently measured according to the initial droplet diameter D_0 and compared to the correlation established by Beckstead [14] in Fig. 3. Each single point represents one measurement following the methodology previously described.

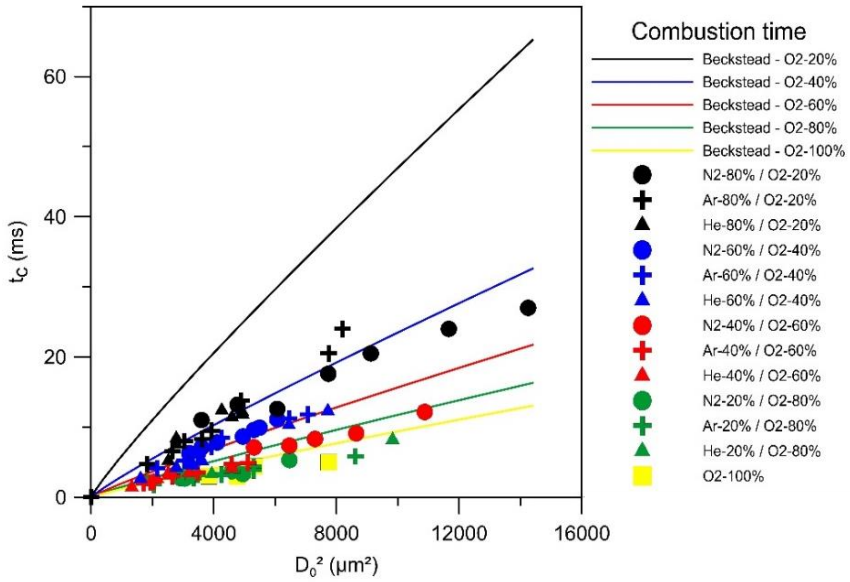

Figure 3. Evolution of the combustion time in several ambient compositions with respect to the square initial particle diameter

A first observation is that the experimental trends are generally in agreement with the correlation but the predictions systematically overestimate the combustion time. Beckstead's correlation is a global fit among many various experimental data and this divergence could be explained by the different experimental conditions used by authors. Nevertheless, results indicate that combustion time evolves almost linearly with the square of the initial droplet diameter and gradually decreases when oxidizer proportions increase, regardless of the diluent

gas. To compare the influence of inert gases N_2, Ar and He, detailed results on combustion time for each dilution ratio are presented in Fig. 4.

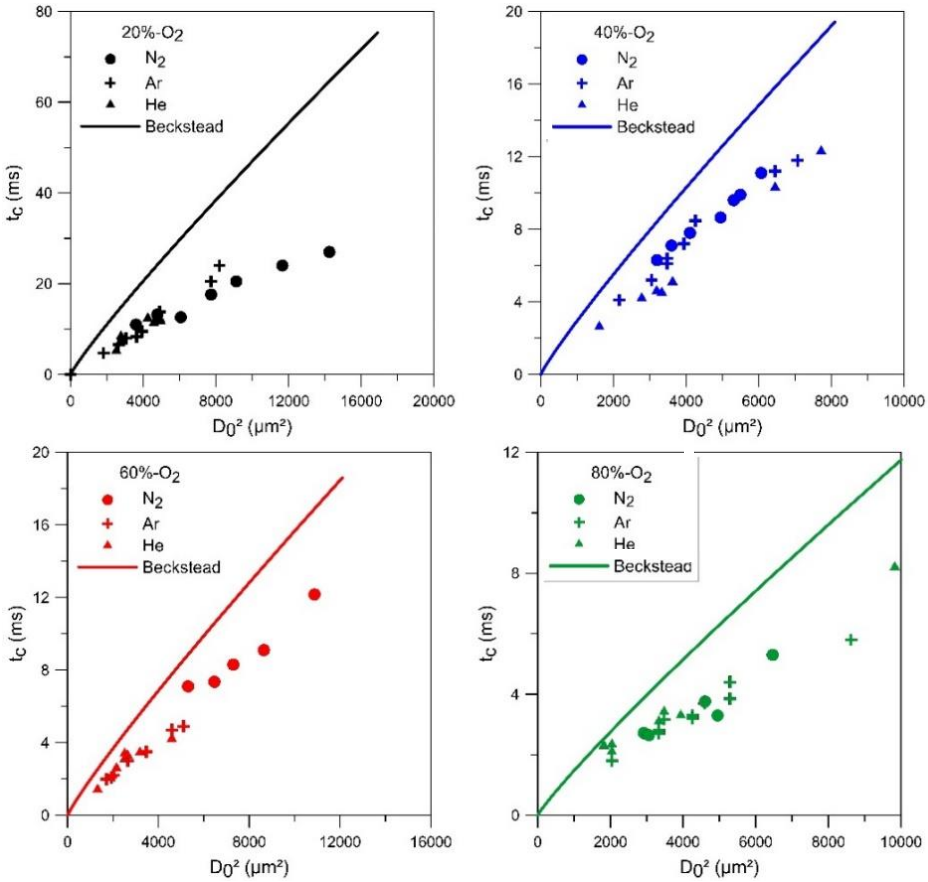

Figure 4. Evolution of the combustion time for different ambient dilution ratio

According to the dataset, the nature of the inert gas does not modify significantly the combustion times which remain similar, even with elevated diluent proportions. This trend confirms reported data from literature. Finally, as considered by Beckstead's correlation, diffusive and thermal properties of the diluent do not have a major effect on the overall combustion of micron-sized aluminum particles and the burning time of a single droplet seems to be driven by the dilution ratio which modifies the reaction rate.

The determination of the burning time exponent is presented in Fig. 5. This calculation is established considering that the aluminum particle totally burns and that the droplet diameter evolves during the overall combustion process following Eq. 1. Using these assumptions, Eq. 2 is deduced with *C* a constant and the exponent *n* is then estimated for each ambient condition.

$$D^n(t) = D_0^n - kt \tag{1}$$

$$n = \frac{\ln t_c}{\ln D_0} + C \tag{2}$$

Data are consistent with documented values. In the cases of argon and helium, trends show that the combustion time is close to the D^2 law for low oxygen contents ($\%O_2 < 40\%$). For dilutions in N_2 and for oxygen-rich mixtures ($\%O_2 > 60\%$), the value of the exponent is lower, indicating that the aluminum combustion process diverges from the theoretical expectations based on the combustion of liquid fuel droplets [15]. Considering the data sensitivity to measurements errors, this interpretation has to be taken with care. The

assumptions are questionable in some cases, particularly for N_2 dilution and high oxygen proportions where a significant part of unburned aluminum was often observed at the end of the combustion process. Analysis of additional parameters is hence required to confirm those results.

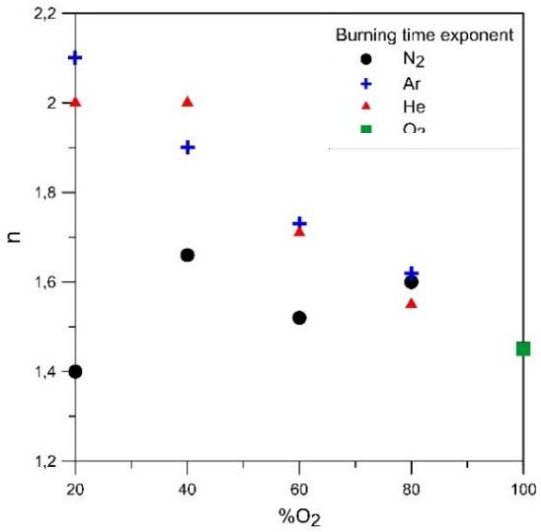

Figure 5. Evolution of the burning time exponent *n* for different ambient conditions

3.2. Aluminum surface regression in symmetric regime

Aluminum consumption rate is an important indicator of the effect of ambient conditions. The regression of the droplet diameter during the symmetric combustion phase is expected to follow a theoretical law as expressed in Eq. 1. Because of the small measurable variation of the droplet diameter on a limited time, especially for N_2, the determination of the exponent *n* is sensitive to measurement errors. Thus, in an attempt to also evaluate the effects of dilution conditions on aluminum consumption in symmetric regime, the comparative method used in this work was based on the classical D^2 law and the exponent *n* was set to 2. Indeed, in the symmetric regime, the droplet surface covered by the oxide lobe is small so that a classical D^2 law is expected to hold. The quantity *k* is a scalar representative of the evaporation rate and defined in Eq. 3. It was experimentally determined using direct visualization for each burning particle. The evaporation rate is constant for given ambient conditions and evolution of k according to the oxygen proportion and the diluent gases is presented in Fig. 6. Each single point represents the average value for a selected diluent gas and error bars indicate the standard deviation. The evaporation coefficient increases for high oxygen contents and the aluminum consumption during the symmetric phase is similar for the different inert gases.

Theoretically, the evaporation process of an isolated burning droplet is driven by heat and mass transfers from the flame to the particle. The heat/mass flux mainly depends on the diffusion properties of the surrounding burning droplet environment. Considering the D^2 law for a Lewis number equal to 1 ($Le \sim 1$), the definition of the Spalding number B_T is given in Eq. 4 and Eq. 5 gives the theoretical expression of the evaporation rate *k* [16]. Gas thermophysical properties (density ρ_s, heat capacity C_p, heat of reaction *Q*, latent heat of vaporization L_v) and diffusion properties (thermal diffusivity α_s) are obtained from thermochemical computations from *NASA Chemical Equilibrium with Applications* (CEA) [17]. Aluminum density ρ_l at high temperatures is taken at 1600 kg/m3. Eq. 4 and 5 are computed for different oxidizer mass fractions $Y_{O\infty}$. Theory is compared to experimental results in Fig. 6 and predicts consistent evaporation rates for dilution with N_2 and Ar and a higher evaporation rate with He. Finally, results are in global accordance with theory, except for combustion in He and for undiluted case. Models or assumptions considered for the theoretical predictions of the evaporation rate according to the D^2 law are possibly limited (high fraction of condensed smoke for undiluted

combustion, $Le \neq 1$ for high dilution in He, etc.). Further investigations will be conducted combining experimental results and numerical simulations to help identify those discrepancies.

$$\left| \frac{d(D^n(t))}{dt} \right| = k \tag{3}$$

$$B_T = \frac{C_p\,(T_\infty - T_s) + (\frac{F}{O})_s\,Y_{O\infty}\,Q}{L_v} \tag{4}$$

$$k = \frac{8\,\rho_s\,\alpha_s\,\ln(1+B_T)}{\rho_l} \tag{5}$$

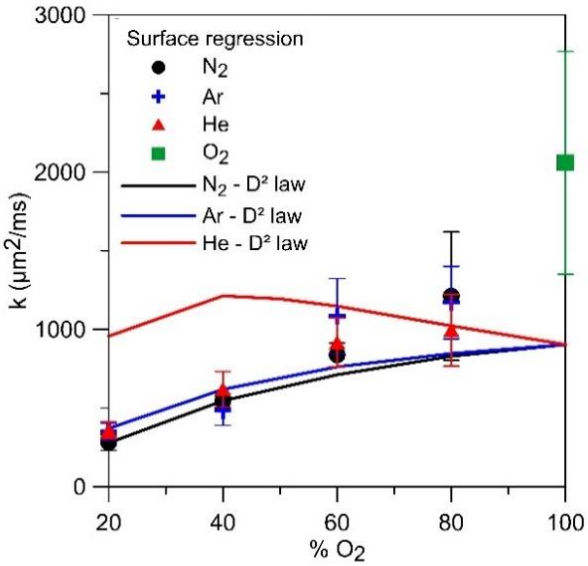

Figure 6. Evolution of the evaporation coefficient k according to the ambient conditions - Measurements and estimates from D^2 law

3.3. Reaction zone

In order to complete information on the effect of the diluent gases on combustion characteristics in the symmetric regime, the position of the flame is analyzed depending on ambient conditions. The flame boundary is optically defined as the brightest border observed in the reaction zone, corresponding to a thermal limit close to the maximum Al_2O_3 mole fraction. This limit is identified analyzing the deconvoluted intensity profile with Abel inversion process. Evolution of the flame radius R_f normalized by the droplet radius R_d was directly measured on each recorded picture with image processing. The quantity R_f/R_d is found to be relatively constant during the combustion in the symmetric regime and independent of the initial droplet diameter. This value is also reproducible for fixed ambient conditions and is represented in Fig. 7 as a function of the oxygen proportion. Each single point represents the average ratio for a selected diluent gas and error bars indicate the standard deviation.

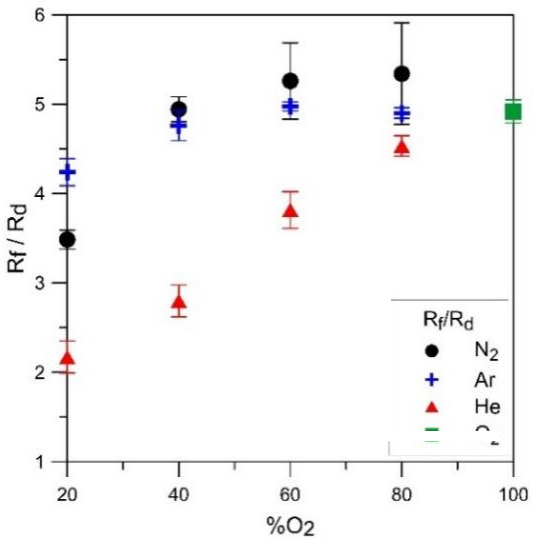

Figure 7. Evolution of the normalized flame radius according to ambient composition

Results show that the variation of the dilution ratio modifies the flame position and the normalized flame radius increases with the oxygen content. The flame is closer to the droplet surface when burning in He and relatively further for N_2 and Ar. These observations corroborate the evolution of the evaporation constant. Indeed, increasing of *k* suggests a higher aluminum mass rate and subsequently, for a given droplet surface, an increased speed of the buoyant flow ejected from the boiling particle. Moreover, according to the data computed with CEA application, mass diffusivity and density of the gaseous components at the droplet surface are nearly constants according to the oxygen proportions. In this case, considering the theoretical approach for a burning droplet in the conditions predicted by the D^2 law [16], the flame size mainly depends on the ratio between the mass rate and the Spalding number which increases for oxygen rich mixtures. Finally, it can explain that the distance between the flame and the burning droplet possibly grows with increasing oxygen fraction. Then, *k* is relatively constant independently of the inert gas and He has a high mass diffusivity compared to N_2 and Ar, justifying the close position of the flame in the case of high dilution in He.

3.4. Regime transition

The characterization of the transition from symmetric to asymmetric phase is essential to evaluate the respective contribution of the different combustion regimes to the overall burning process. This transition is visually defined when the flame shape is modified (Fig. 9 (a) 3), also corresponding to a specific increase in light emission. The regime transition was identified with N_2, Ar and He for low and high dilution contents. However, the duration of the symmetric phase t_{avp} and the droplet diameter at transition occurrence D_{avp}, respectively scaled by the combustion time t_c and initial droplet diameter D_0, depend both on the inert gas and its relative proportions. Their evolution is exposed in Fig. 8. Each single point corresponds to the average of the relative values for a selected diluent gas and error bars indicate the standard deviation.

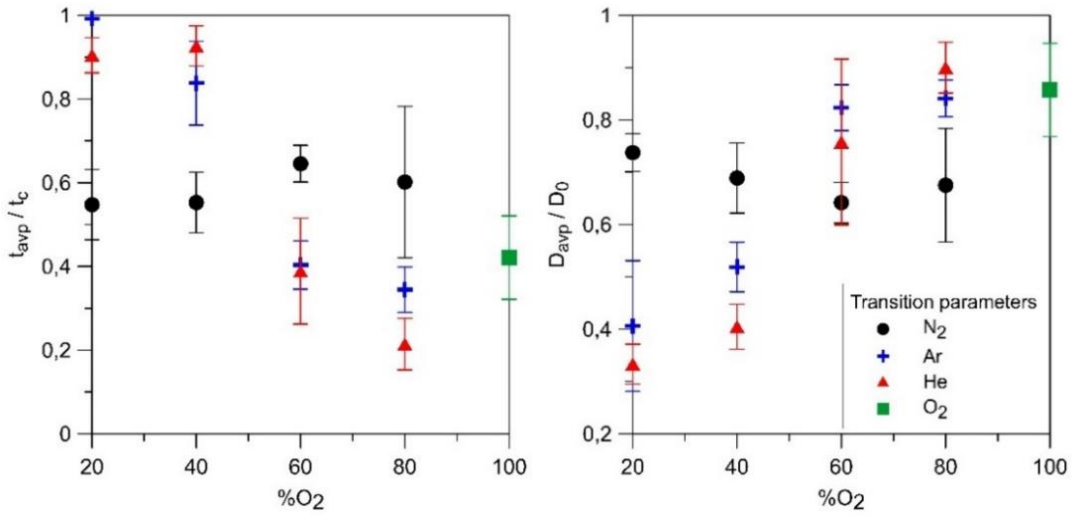

Figure 8. Effect of the dilution conditions on the regime transition

In the case of high dilution levels, where the effect of the diluent gases is noticeable, the presence of N_2 contributes in decreasing the duration before regime transition compared to Ar and He. Evaluation of D_{avp} also corroborates this expectation and the droplet diameter before transition in N_2 is relatively larger (Fig. 8). For combustion with high dilution in Ar and He, transition occurs close to the end of the burning process when the aluminum particle is almost totally consumed, meaning that the combustion is symmetric all the way through. (Fig. 8). Thus, the diluent gases are identified to have respective influences on the combustion process for high dilution ratio ($\%O_2 < 40\%$). On the opposite, this trend is then less marked for low dilution ratio where the effects of N_2, Ar and He are restrained. Considering the data scatter for high oxygen fraction ($\%O_2 > 60\%$), the transition parameters become mainly driven by the relative oxygen content and the different inert gases are supposed to have a weak effect. A specific trend has to be noticed when burning in N_2 atmosphere with constant transition parameters, irrespective of the dilution level.

Combustion processes for high dilution in N_2, Ar and He are illustrated in Fig. 9. For each case (a), (b) and (c), left pictures are raw unprocessed and a Laplacian filter is applied to the right pictures to highlight the oxide lobe evolution. This image processing approximates the second derivative in both directions of the picture which is then represented as a gray-scale image to allow the contour detection. The oxide lobe corresponds to the brighter zone on non-processed pictures and is colored (red) on the filtered images.

Different changes in oxide lobe size are observed depending on the inert gas considered in oxygen-lean mixtures. Accumulation of oxide on the droplet surface is noticed for particles burning in N_2/O_2 (Fig. 9 (a)). Because of the accumulation process, the droplet is quickly partially or totally covered by the oxide lobe, generating an early regime transition (Fig. 9 (a) 2-3). For other inert gases, the volume of the oxide cap remains limited and more or less constant, approximately equal to the volume of the initial molten alumina layer (Fig. 9 (b)-(c)). Nonetheless, during the combustion process, the relative surface covered by the initial oxide lobe increases with the droplet size reduction and becomes finally important enough to trigger a late transition (Fig. 9 (b)-(c) 3).

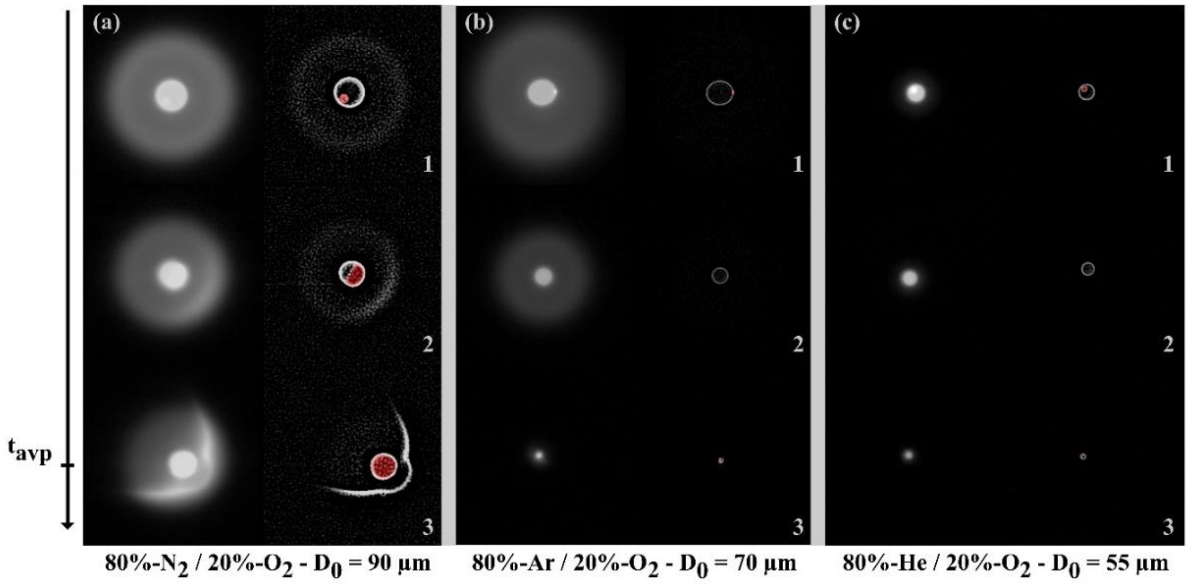

Figure 9. Video pictures of the combustion process for high diluted ambient conditions – Oxide lobe in red

For low dilution, the size of the oxide lobe is observed to increase regardless of the diluent. Furthermore, Fig. 10 presents the combustion process of an aluminum particle burning in an environment containing only O_2. The upper images are unprocessed and a Laplacian filter is applied on the lower picture, allowing to distinguish the oxide lobe (red) and the smoke products (orange). As observed, in undiluted conditions, condensed smoke products can be directly transported to the burning particle (Fig. 10 1-2-3) and impact the droplet surface (Fig. 10 4). The oxide lobe size is clearly modified by this process and grows significantly on the reactive surface (Fig. 10 3-5), shifting the combustion regime. In this case, it seems that significant lobe formation results from direct transport of condensed oxide from the flame.

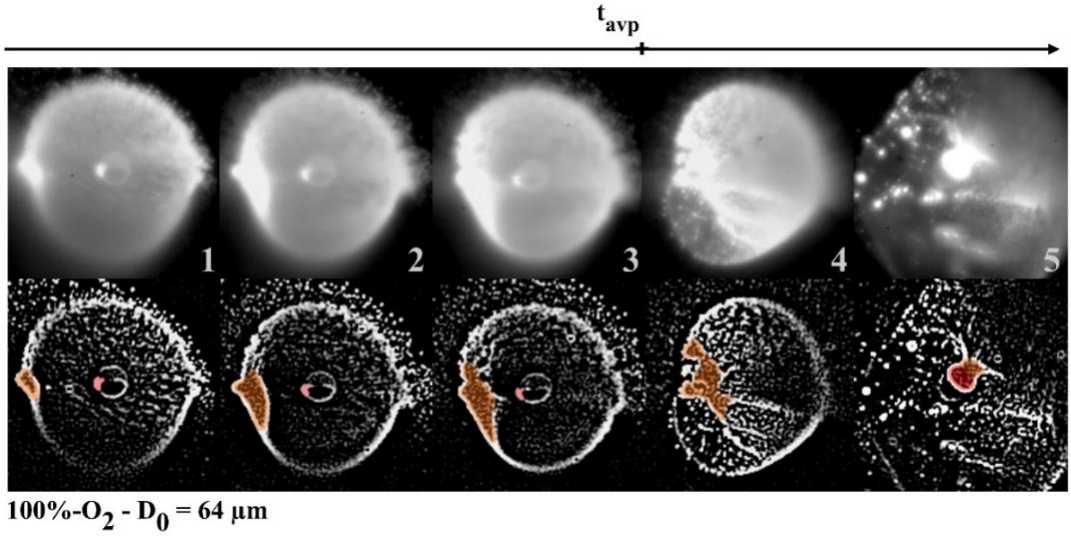

Figure 10. Video pictures of the combustion process in an undiluted environment

4. Discussion

Various trends on the relative effect of non-reactive species are identified. Based on reported data and different assumptions, contributions of the diluent gases in aluminum combustion process, especially on transport mechanisms, can be described.

First, even if analysis of the combustion time does not highlight a potential influence of the diluent gases, modification of the burning time exponent *n* is a first indicator on the respective roles of N_2, Ar and He. Indeed, in the case of aluminum combustion, modification of the exponent *n* can be attributed to the accumulation of condensed oxide and subsequent lobe formation on the droplet surface [14]. Thus, values of *n* (*n*~2*)* for high dilution in Ar and He suggests that those ambient conditions limit the oxide production or diffusion back to the droplet. Conversely, the reduction of the burning time exponent in the case of dilution in N_2 or for high oxygen contents ($\%O_2 > 60\%$) could indicate that expansion of an oxide lobe on the droplet surface is sufficiently considerable to alter the combustion process.

The trends of the aluminum evaporation rate according to the oxygen proportions for the different inert gases are in a relative accordance with theoretical expectations, meaning that the combustion process in symmetric regime probably follows the D^2 law. The variation of *n* can hence be attributed to the regime transition and to the inherent lobe formation. Moreover, considering the lower value of the burning time exponent for combustion with N_2 compared to Ar and He for high dilution levels, the accumulation of oxide is supposed to be more important. However, this process reduces the surface available for aluminum evaporation and can potentially decrease the evaporation rate. Estimations of *k* for N_2 and Ar do not account for this assumption, indicating a fast expansion of the oxide lobe on the droplet surface and supporting the theory of the reported transition mechanism [7].

Investigations on the transition phase reported that the presence of N_2 contributes to an earlier modification of the combustion regime. Considering that the regime transition is driven by the accumulation of aluminum oxide and lobe formation on the droplet surface, those results could be consistent with the assumption of the formation of low reactive NO species which may contribute to transport oxygen from the flame to the droplet [8]. This phenomenon is especially notable for important N_2 proportions where potential NO formation is considerably favored, generating fast production of condensed alumina on the droplet surface by heterogeneous reaction with aluminum [9]. In high fractions of Ar and He, transition regime occurs tardily and the accumulation of oxide on burning droplets is not observed, suggesting that transport of O, O_2 and suboxides to the reacting surface is limited or even inhibited, probably due to their high reactivity.

Various mechanisms can drive the transport of both condensed oxide and oxygenated species from the flame to the burning droplet, leading to oxide lobe expansion. Diffusiophoresis and thermophoresis can possibly allow the transport of small condensed oxide particles to the droplet surface (Fig. 10) and gaseous oxygen-containing molecules can reach the molten aluminum by diffusion. The comparison between dilution in Ar and in He is interesting to evaluate respective contributions of those phenomena. Adiabatic flame temperatures are relatively analogous and equilibrium speciations are the same but dilution in He promotes a highly diffusive environment ($D_{O2/He}/D_{O2/Ar} \sim 4$) which potentially contributes to the species transport. Nonetheless, results on transition parameters do not indicate any significant disparity and therefore, the diffusive effects (diffusiophoresis and mass diffusion) do not appear to be processes governing oxide lobe formation.

Following those observations and data, it is also interesting to note that the burning time is not altered by the variation of the transition parameters for a given dilution ratio. The evaporation rate is expected to dramatically decrease in the asymmetric phase because of the reduced reacting surface, that is why a modification on the trend of the burning time could be expected for combustion in N_2 compared to Ar and He, especially for high diluent proportions. Qualitative observations made with high-speed camera suggest an important quantity of unburned aluminum in the case of an early transition regime, possibly justifying that the overall combustion time is reduced compared to the expectations.

Correlating the accumulation process of oxygenated products on the droplet surface with the transition parameters requires complementary data. Indeed, observations in various conditions indicate that the oxide lobe could be more or less spread on the droplet surface and composition of the oxide cap can be strongly dependent on the temperature history [7]. The regime transition is assumed to be associated with the relative covered surface by the oxide lobe and is supposed to occur when a threshold coverage is reached, so that surface tension of the oxide lobe could also be decisive. In these conditions, investigations on the dependence of the oxide lobe composition and its surface tension to the temperature has to be extended.

5. Conclusion

The contribution of N_2 diluent in the combustion of a single aluminum particle in O_2 atmosphere has been analyzed in an experimental study and compared with Ar and He, investigating several combustion parameters. These diluents were also selected to highlight the relative influence of heat capacity, diffusivity or thermal conductivity on the combustion process in diffusion mode.

Overall, regardless of the inert gas, dilution reduces temperatures and aluminum consumption rate, resulting in a flame closer to the droplet and a longer combustion time. The combustion dynamics is also modified. A high oxygen proportion surrounding the particle is assumed to enhance the transport of oxygenated species from the flame to the particle, contributing to a quick formation and accumulation of aluminum oxide on the droplet surface. Moreover, additional direct transport of condensed smoke particles can potentially occur, feeding the oxide lobe. Hence, the duration of the symmetric combustion regime is found to decrease when the ratio of oxidizer increases.

It was found that intrinsic properties of the diluent gases do not have a significant effect on combustion characteristics. Indeed, only the position of the flame was found to be dependent on the diluent characteristics. However, the modification of the inert gas is likely to alter the symmetric/asymmetric transition parameters. In same proportions, transition regime occurs relatively earlier for dilution with N_2 due to the important expansion of the oxide cap. Thus, these observations and data are consistent with the transport mechanism which assumes that the formation of low reactive NO species enhances the oxygen supply inward the droplet, contributing to heterogeneous reactions. The evaporation rate during the symmetric phase also remains similar for N_2, Ar and He, indicating that accumulation of oxide on the droplet surface either does not restrain the fuel evaporation or is not progressive but rather sudden. Otherwise it was note that the burning time is not altered by the variation of the symmetric phase duration despite theoretical expectations. Then, High diffusivity of He was assumed to enhance the oxygen diffusion to the particle, but, according to the similarities of the combustion dynamics in Ar and He, diffusivity of the diluent gas does not appear as a significant parameter. Thus, the main mechanism for oxygen transport is likely the thermophoresis of oxygen-containing species produced in the flame.

To conclude, a new dataset on aluminum combustion in O_2/diluent mixtures was provided and some assumptions were supported or discussed. These data have to be considered for the selected and representative particle size range. Contribution of some mechanisms can be potentially different in the case of coarser particles (diffusion, thermophoresis, conduction, etc.). The independence of the burning time on the variations of the combustion dynamics remains interesting and has to be further explained by future works. Investigations on the accumulation process of oxide on the droplet surface has to be extended. Quantitative estimations of the oxide lobe size evolution during combustion could improve the understanding. Furthermore, information is required on chemical composition and surface tension of the oxide lobe according to the temperature history during the combustion process to confirm the relevance of the interpretations made in this work.

References

[1] S. Gallier, F. Godfroy, Aluminum Combustion Driven Instabilities in Solid Rocket Motors, J. Propul. Power 25 (2009) 509-521

[2] M.W. Beckstead, R.L. Derr, C.F. Price, A model of composite solid-propellant combustion based on multiple flames, AIAA Journal 8(12) (1970) 2200-2207

[3] E.L. Dreizin, Experimental study of stages in aluminium particle combustion in air, Combust. Flame 105(4) (1996) 541-556

[4] A. Braconnier, C. Chauveau, F. Halter, S. Gallier, Detailed analysis of combustion process of a single aluminum particle in air using an improved experimental approach, International Journal of Energetic Materials and Chemical Propulsion 17(2) (2018) 111-124

[5] R. Friedman, A. Maček, Ignition and combustion of aluminium particles in hot ambient gases, Combust. Flame 6 (1962) 9-19

[6] J.L. Prentice, L. Nelson, 1967, Differences between the combustion of aluminum droplets in air and in an oxygen-argon mixture, Naval Weapons Center, China Lake, California.

[7] E. Dreizin, Effect of Phase Changes on Metal-Particle Combustion Processes, Combust. Explo. Shock+ 39(6) (2003) 681–693

[8] E.L. Dreizin, On the mechanism of asymmetric aluminum particle combustion, Combust. Flame 117(4) (1999) 841-850

[9] E.L. Dreizin, Experimental study of aluminum particle flame evolution in normal and micro-gravity, Combust. Flame 116(3) (1999) 323-333

[10] P. Bucher, R.A. Yetter, F.L. Dryer, E.P. Vicenzi, T.P. Parr, D.M. Hanson-Parr, Condensed-phase species distributions about Al particles reacting in various oxidizers, Combust. Flame 117(1–2) (1999) 351-361

[11] J.L. Prentice, 1974, Aluminum droplet combustion: rates and mechanisms in wet and dry oxidizers, Naval Weapons Center, China Lake, CA.

[12] V. Sarou-Kanian, J.C. Rifflet, F. Millot, G. Matzen, I. Gökalp, Influence of nitrogen in aluminum droplet combustion, Proceedings of the Combustion Institute 30(2) (2005) 2063-2070

[13] A. Zenin, G. Kusnezov, V. Kolesnikov, Physics of aluminum particle combustion at convection, Proc. 38th Aerospace Sciences Meeting and Exhibit, American Institute of Aeronautics and Astronautics, (2000).

[14] M. Beckstead, 2004, A summary of aluminum combustion, Brigham Young Univ Provo Ut.

[15] I. Glassman, 1959, Metal combustion processes, Princeton Univ NJ James Forrestal Research Center, Princeton, New Jersey.

[16] K.K. Kuo, Principles of combustion, (2005).

[17] B.J. McBride, Computer program for calculation of complex chemical equilibrium compositions and applications, NASA Lewis Research Center, (1996).